# ChemComm

## Accepted Manuscript

This article can be cited before page numbers have been issued, to do this please use: N. Nishitani, T. Hirose and K. Matsuda, *Chem. Commun.*, 2019, DOI: 10.1039/C9CC02093D.


This is an Accepted Manuscript, which has been through the Royal Society of Chemistry peer review process and has been accepted for publication.

Accepted Manuscripts are published online shortly after acceptance, before technical editing, formatting and proof reading. Using this free service, authors can make their results available to the community, in citable form, before we publish the edited article. We will replace this Accepted Manuscript with the edited and formatted Advance Article as soon as it is available.

You can find more information about Accepted Manuscripts in the author guidelines.

Please note that technical editing may introduce minor changes to the text and/or graphics, which may alter content. The journal's standard Terms & Conditions and the ethical guidelines, outlined in our author and reviewer resource centre, still apply. In no event shall the Royal Society of Chemistry be held responsible for any errors or omissions in this Accepted Manuscript or any consequences arising from the use of any information it contains.

ROYAL SOCIETY OF CHEMISTRY

rsc.li/chemcomm

ROYAL SOCIETY OF CHEMISTRY View Article Online
DOI: 10.1039/C9CC02093D

Journal Name

COMMUNICATION

# Self-Assembly of Photochromic Diarylethene–Peptide Conjugates Stabilized by β-Sheet Formation at the Liquid/Graphite Interface†

Nobuhiko Nishitani,[a] Takashi Hirose[b] and Kenji Matsuda*[a]

Received 00th January 20xx,
Accepted 00th January 20xx

DOI: 10.1039/x0xx00000x

www.rsc.org/





**Two-dimensional (2-D) self-assembly of diarylethene (DAE)–peptide conjugates at the octanoic acid/graphite interface was investigated by scanning tunneling microscopy (STM). The open-ring isomer of a DAE–peptide conjugate formed a stable 2-D molecular assembly with an antiparallel β-sheet structure. Quantitative analysis of surface coverage depending on concentrations revealed a stronger stabilization effect of oligopeptide than that of alkyl group with similar side chain length.**

Three-dimensional structure of proteins is closely related to the sophisticated functions of biomolecules, which originates from composition and sequence of amino acids.[1–3] The motif of self-assembly seen in biomolecules has been used to create artificial supramolecular systems such as those consisting of π–peptide conjugated molecules.[4–11]

Self-assembly on surface is a powerful approach to construct functionalized two-dimensional (2-D) nano-architectures.[12–14] Oligopeptides should be a promising building blocks not only for 3-D systems but also for 2-D self-assemblies. De Feyter, Meijer, Schenning, and co-workers reported a pioneering work on 2-D self-assembly of π-conjugated molecules bearing oligopeptide in 2008, in which the formation of an antiparallel β-sheet was clearly visualized by scanning tunnelling microscopy (STM) with the single-molecule resolution.[15] Recently, Wang et al. have reported systematic studies on conformational dynamics and site-specific analysis of amyloid β peptides using STM since 2012.[16–22] Direct visualization of the bioinspired 2-D self-assemblies has been widely investigated using STM, however, the stabilization energy of 2-D assemblies by the formation of hydrogen bonding structures of oligopeptide has not been discussed quantitatively.

Photochromic compounds are key molecular components of photoresponsive 2-D self-assemblies that can be utilized as optoelectronic nanodevices working at the molecular level.[23,24] We have previously reported photochromic diarylethenes (DAEs) showing a phototriggered multi-state ordering transformation at the liquid/graphite interface, where 2-D ordering domains composed of one isomer of DAE were replaced by different domains of the other isomer upon light irradiation.[25–29] On the other hand, photoswitching of individual molecules at the single-molecule level with keeping the original ordering domains has not been achieved, likely due to fast exchange of molecular components; the photoisomerized isomer in a 2-D ordering is likely exchanged with the original isomer via adsorption/desorption dynamics at the liquid/solid interface.

According to the literature, STM observation of the single-molecule-level photoswitching is limited to only self-assembled monolayer (SAM) on Au(111) surfaces[30,31] and vapor-deposited monolayer under ultra-high vacuum (UHV) conditions,[32–34] where exchange of molecular components is restricted. We envision that slow adsorption/desorption dynamics is a necessary condition to observe single-molecule switching at liquid/solid interfaces with keeping the original 2-D ordering domains.

Herein, we report the synthesis of DAE–peptide conjugates and their 2-D self-assembly at the liquid/graphite interface (Figure 1). We found that the DAE–peptide conjugate, having both oligopeptide and hexadecyl chains, formed a stable 2-D molecular assembly, which was stabilized by the antiparallel β-sheet structure of oligopeptide moieties. A strong stabilization effect of the formation of antiparallel β-sheet on 2-D self-assembly was successfully quantified by the analysis of surface coverage depending on concentration changes.

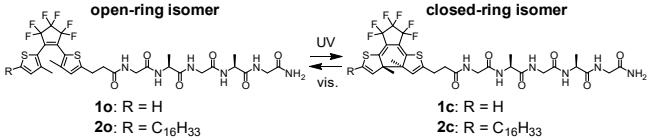


**Figure 1.** (a) Chemical Structures and photochromic reaction of DAEs **1** and **2**.

[a] *Department of Synthetic Chemistry and Biological Chemistry, Graduate School of Engineering, Kyoto University, Katsura, Nishikyo-ku, Kyoto 615-8510, Japan. E-mail: kmatsuda@sbchem.kyoto-u.ac.jp*
[b] *Institute for Chemical Research, Kyoto University, Uji, Kyoto 611-0011, Japan.*
† Electronic Supplementary Information (ESI) available: Experimental procedures, additional STM images, and $^{1}H$ and $^{13}C$ NMR spectra. See DOI: 10.1039/x0xx00000x

Diarylethenes **1o** and **2o** were synthesized using a solid-phase peptide synthesis (see the ESI). Glycyl-alanyl sequence (Gly-Ala-Gly-Ala-Gly, GAGAG) is the key repeating motif for the β-sheet structure in silk fibers,[35,36] which was commonly introduced to **1o** and **2o**. In addition, a hexadecyl chain was introduced into **2o** to enhance the affinity to the graphite surface. The GAGAG peptide bearing *N*-terminated amine was prepared by Fmoc solid-phase synthesis. Solid-phase coupling of GAGAG peptide with carboxylic acid derivatives of DAEs, and subsequent cleavage from the resin provided **1o** and **2o** in 68% and 47% yield, respectively. The synthetic details and characterization using NMR spectroscopy and mass spectrometry are shown in Supporting Information (ESI).

Photoisomerization reaction of **1** and **2** was investigated in octanoic acid by UV-vis absorption spectroscopy (Figures 2a and S1). The open-ring isomers **1o** and **2o** showed absorption bands at 336 and 343 nm, respectively. The molar extinction coefficient ($\varepsilon$) was 1.2 × $10^4$ $M^{-1}cm^{-1}$ at the maximum absorption wavelength both for **1o** and **2o**. The magnitude of absorption spectra was linearly increased with increasing concentration at concentrations of 40 μM or less, and showed a negative deviation from linearity at 100 μM, suggesting that **1o** and **2o** did not form any aggregate at concentrations of 40 μM or less in octanoic acid (Figures S2 and S3).

Upon irradiation with UV light (313 nm) to an octanoic acid solution of **2o**, new absorption band appeared at 435 nm, suggesting the photoisomerization from the open-ring isomer **2o** to the closed-ring isomer **2c**. The original spectrum of **2o** was fully restored by successive irradiation with visible light (> 460 nm), indicating a reversible photoisomerization reaction. The closed-ring isomer **2c** could not be isolated by HPLC. Instead, assuming the molar extinction coefficient of **2c** is identical to a reference compound, i.e., 1,2-bis(3,5-dimethyl-3-thienyl)perfluorocyclopentene ($\varepsilon$ = 5.8 × $10^3$ $M^{-1}cm^{-1}$ at 425 nm in hexane),[37] the conversion ratio of **2c** to **2o** at the photostationary state (PSS) was estimated to be around 85% in octanoic acid.

Self-assembly of **1o** and **2o** in solution phase was detected by circular dichromism (CD) spectroscopy (Figures 2b and S4). **1o** and **2o** showed a negative Cotton effect at 320–340 nm at 100 μM or higher in octanoic acid, whereas no CD signal was observed for **2o** under dilute conditions, i.e., 40 μM or less, which was consistent with concentration dependence of

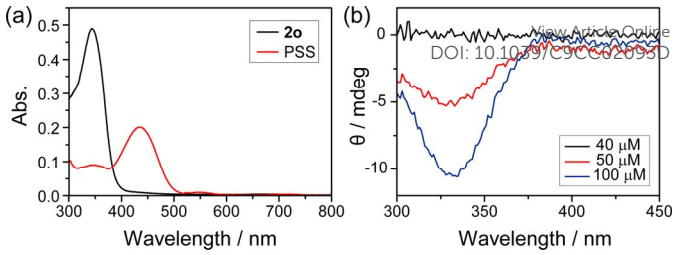


**Figure 2.** (a) UV-vis. spectral change of **2** in octanoic acid upon photoisomerization ($c$ = 40 μM, cell length: 10 mm). (b) CD spectra of **2o** in octanoic acid (cell length: 2 mm).

absorption spectra. Considering that CD signal was observed at 320–340 nm where oligopeptide has no absorption, diarylethene core moiety of **1o** and **2o** took a chiral conformation in aggregates induced by the chiral peptide chain.

The manner of 2-D ordering of **1o** and **2o** was investigated by STM at the octanoic acid/highly oriented pyrolytic graphite (HOPG) interface. Octanoic acid solution of **1o** or **2o** was deposited on a freshly cleaved HOPG substrate, and then STM image was recorded at the liquid/solid interface. No ordering was observed for **1o** at concentrations of 200 μM or less (Figure S5a). Although 2-D orderings was detected using saturated solution of **1o**, the detailed structure was unfortunately not clear (Figure S5b).

In contrast, a clear stripe-patterned ordering of **2o** was recorded at 200 μM (Figure 3a), suggesting that hexadecyl chain has an important role to stabilize 2-D ordering at the liquid/HOPG interface. According to high-resolution STM images of **2o**, the lattice parameters were determined as $a$ = 5.8 ± 0.1 nm, $b$ = 0.96 ± 0.02 nm, $\alpha$ = 87 ± 1°, from which the unit area occupied by one molecule of **2o** on surface was determined as $S$ = 2.80 ± 0.14 $nm^2$ (Figure 3b). The stripe-patterned ordering was well reproduced by the molecular mechanics/molecular dynamics (MM/MD) calculations, suggesting that oligopeptide chain of **2o** took an antiparallel β-sheet structure in the 2-D ordering, where methyl group of alanine extended to the liquid phase to avoid collision with the substrate (Figure 3c). It is noted that DAE core of **2o** took a photoactive antiparallel conformation, therefore, photoisomerization reaction from the open- to the closed-ring isomer is possible in 2-D self-assembly. The formation of antiparallel β-sheet conformation is consistent with the previous report by De Feyter et al., in which a similar pattern of

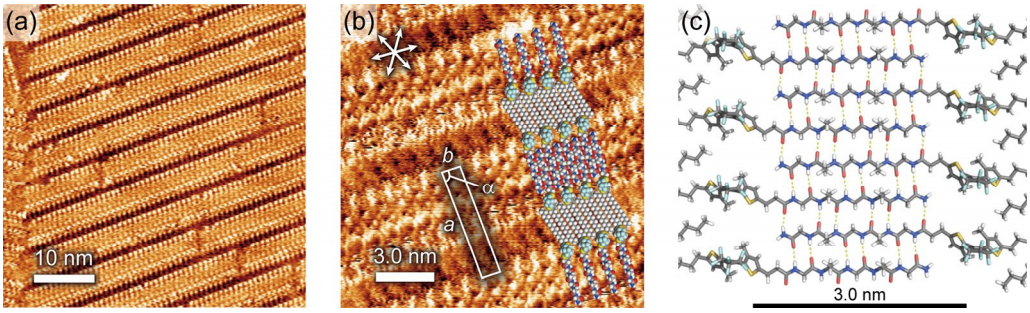


**Figure 3.** (a) STM images of **2o** at the octanoic acid/HOPG interface ($c_t$ = 200 μM, $I_{set}$ = 10 pA, $V_{bias}$ = −800 mV). (b) High-resolution STM image of molecular ordering of **2o** at the octanoic acid/graphite interface ($c_t$ = 200 μM, $I_{set}$ = 40 pA, $V_{bias}$ = −800 mV) and the molecular model of **2o** simulated by MM/MD calculations. (c) Enlarged image of the molecular model showing the formation of antiparallel β-sheet conformation composed of GAGAG oligopeptide sequence. Yellow dotted line denotes the six-fold hydrogen bond network.

2-D ordering was observed for a oligo(*p*-phenylenevinylene) derivative with GAGAG oligopeptide at the liquid/HOPG interface.[15]

The stabilization effect of the formation of antiparallel β-sheet structure was quantitatively analyzed for the first time in this study. The surface coverage of **2o** depending on the change of concentration was observed by STM (Figure 4). The mean value of surface coverage at a concentration was determined by 15 STM images recorded at different places on HOPG substrate (Table S1). Note that the surface coverage observed by STM was stable at least during several hours after the sample deposition. As shown in Figure 4b, **2o** showed a steep increase of surface coverage with increasing concentration. We noticed that concentration for the 2-D ordering formation of **2o** was similar to that for the aggregation in solution phase, i.e., ca. 50 μM in octanoic acid according to concentration dependence of CD spectra (Figure 2b).

A 2-thienyl-type DAE **3o** bearing two of *N*-tetradecylcarbamoylethyl groups composed of totally 36 non-hydrogen atoms ($C_{34}N_2$) in the main chain, was used as a reference compound.[40] The length of side chains of **3o** is similar to that of **2o** composed of totally 35 non-hydrogen atoms ($C_{29}N_6$) for the two chains. The critical concentration ($c_{crit}$), defined as the concentration at which surface coverage saturates, of **2o** ($c_{crit}$ = 70 μM) was significantly smaller than that of **3o** ($c_{crit}$ = 2000 μM), suggesting that the ordering **2o** was strongly stabilized by the formation of antiparallel β-sheet.

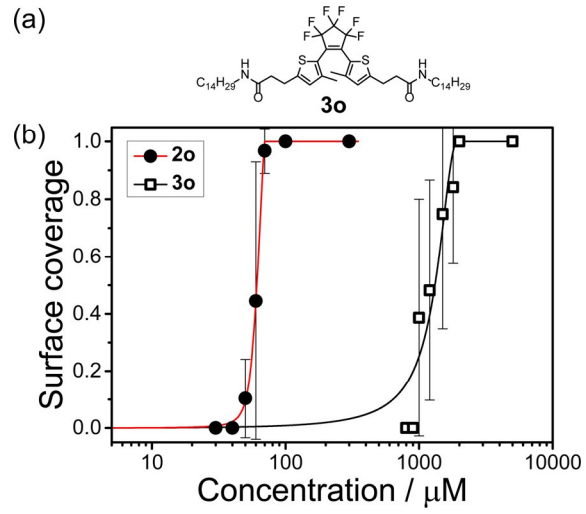


**Figure 4.** (a) Chemical Structure of diarylethene **3o**. (b) Concentration dependence of surface coverages of **2o** and **3o** at the octanoic acid/graphite interface. The red and black solid lines denote the best-fit curves simulated by the nucleation–elongation model. Data points for **3o** were taken from ref 40.

The experimental plots of surface coverage were successfully reproduced by the nucleation–elongation model for 2-D self-assembly at the liquid/solid interface that was developed by our group.[27,28,38–43] According to our model, the surface coverage ($\theta$) can be described as follows:

$$\theta = (1-\theta)\cdot\frac{\sigma K_e(c_t-\alpha\theta)}{\{1-K_e(c_t-\alpha\theta)\}^2} \quad , \quad \alpha = \frac{A_{sub}}{L\cdot N_A\cdot S} \qquad (1)$$

where $K_n$ and $K_e$ are the nucleation and elongation equilibrium constants, respectively, and $\sigma$ is the degree of cooperativity defined as the ratio of two equilibrium constants ($K_n/K_e$). By non-linear regression analysis using eq 1, optimized adsorption parameters $K_n$ and $K_e$ of **2o** were determined as $K_n = 60 \pm 60$ $M^{-1}$ and $K_e = (1.7 \pm 0.1) \times 10^4$ $M^{-1}$, respectively. The $\sigma$ value of **2o** was calculated as $\sigma = (4 \pm 4) \times 10^{-3}$ from the two equilibrium constants. The Gibbs free energy for adsorption in elongation processes ($\Delta G_e$) was calculated according to the equation $\Delta G_e = -RT \ln K_e$, in which $R$ is the gas constant and $T$ is the temperature. The $\Delta G_e$ value for **2o** (−24.1 kJ $mol^{-1}$) was negatively larger by 8.6 kJ $mol^{-1}$ than that of **3o** (−15.5 kJ $mol^{-1}$), suggesting that oligopeptide moieties of **2o** has a significant stabilization effect on the formation of 2-D self-assembly compared with that of alkyl chain moieties of **3o**. According to MM calculations, the energy of lateral intermolecular interaction ($E_{mol-mol}$), which is the sum of van der Waals and hydrogen bond interactions, for **2o** was negatively larger than that of **3o** by 60.6 kJ·$mol^{-1}$ (Figure S13 and Tables S2–S5), suggesting that the negatively larger $\Delta G_e$ value of **2o** than that of **3o** is attributed to the large intermolecular interaction of oligopeptide chains in the 2-D molecular ordering.

According to our previous reports on the size of 2-D ordering domains, the domain size tended to be small for compounds showing an isodesmic-type self-assembly process (i.e., the $\sigma$ value is close to 1),[38,41] whereas the large domain size was commonly observed for compounds showing highly cooperative self-assembly processes (i.e., $\sigma << 1$) whose domain sizes were typically larger than the maximum scan size of STM providing molecular resolution (~500 × 500 $nm^2$).[27,38,40,41,43] It is noted that the domain size of **2o**, showing the small $\sigma$ value of $4 \times 10^{-3}$, was remarkably small (~100 × 100 $nm^2$) even when the surface coverage was not saturated ($c_t$ = 50 μM, Figure S8). The size of 2-D ordering domains is likely related to the nucleation process at the liquid/solid interface. The small domain size of **2o** may be attributed to the fast nucleation rate and/or slow adsorption/desorption dynamics at the liquid/solid interface.

Next, the mixing of the closed-ring isomer **2c** in the 2-D domain composed of **2o** was examined by STM. UV light (313 nm) was irradiated before the deposition on HOPG substrate to prepare a mixed solution of **2o**/**2c** (= 60/40) ($c_t$ = 200 μM). As shown in Figure 5, the resolution of STM image significantly decreased compared to that of pure **2o** (Figure 3a), and some

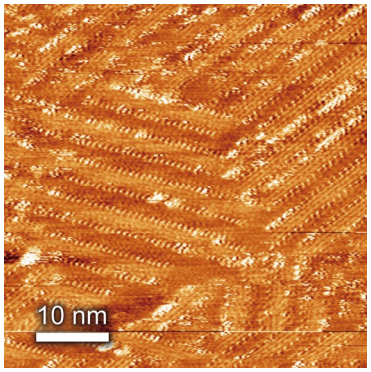


**Figure 5.** The STM image of a mixture of **2o**/**2c** (60/40) at the octanoic acid/HOPG interface ($c_t$ = 200 μM, $I_{set}$ = 10 pA, $V_{bias}$ = −800 mV).

parts of DAE core moiety in the 2-D ordering were found to have a brighter contrast than the others after UV light irradiation. However, it is difficult to conclude the generated brighter parts to be mixed adsorption of **2c** or multi-layer adsorption of **2o** from this experimental result using STM. The further study for photoisomerization reaction in 2-D ordering is currently under investigation in our group.

In conclusion, we reported the solid-phase peptide synthesis and self-assembly behavior of DAE–peptide conjugates at the liquid/graphite interface. The DAE–peptide conjugate having a hexadecyl chain formed a stable 2-D molecular assembly at the octanoic acid/graphite interface. Oligopeptide moieties formed an antiparallel β-sheet structure and DAE core moieties took photoactive antiparallel conformation at the 2-D interface. Quantitative analysis of surface coverage depending on concentrations revealed that oligopeptides are useful molecular motifs to construct stable 2-D molecular orderings, i.e., the critical concentration for the formation of 2-D ordering can be decreased by more than one order of magnitude by replacing alkyl side chain with GAGAG oligopeptide having a comparable chain length. The molecular design strategy in this work will provide a key concept for fabrication of photo-functional 2-D molecular assembly which works at the single-molecule level.

This work was supported by JSPS KAKENHI Grant Numbers JP26107008, JP18K05077, and JP17J10353 from the MEXT, Japan. N. N. acknowledges the LIMS program from the MEXT, Japan. We thank Dr. Tomonori Tamura and Prof. Itaru Hamachi (Graduate School of Engineering, Kyoto University) for assistance with the solid-phase peptide synthesis, and Prof. Michinori Suginome (Graduate School of Engineering, Kyoto University) for providing a microwave peptide synthesizer.

## Conflicts of interest

There are no conflicts to declare.

## Notes and references

1 P. Y. Chou, G. D. Fasman, *Biochemistry* **1974**, *13*, 222–245.
2 C. K. Smith, L. Regan, *Science* **1995**, *270*, 980–982.
3 L. Regan, D. Caballero, M. R. Hinrichsen, A. Virrueta, D. M. Williams, C. S. O'Hern, *Pept. Sci.* **2015**, *104*, 334–350.
4 Y. Matsuzawa, K. Ueki, M. Yoshida, N. Tamaoki, T. Nakamura, H. Sakai, M. Abe, *Adv. Funct. Mater.* **2007**, *17*, 1507–1514.
5 A. Jatsch, E.-K. Schillinger, S. Schmid, P. Bäuerle, *J. Mater. Chem.* **2010**, *20*, 3563–3578.
6 S. H. Kim, J. R. Parquette, *Nanoscale* **2012**, *4*, 6940–6947.
7 J. D. Tovar, *Acc. Chem. Res.* **2013**, *46*, 1527–1537.
8 H. A. M. Ardoña, J. D. Tovar, *Bioconjugate Chem.* **2015**, *26*, 2290−2302.
9 N. Kameta, M. Masuda, T. Shimizu, *Chem. Eur. J.* **2015**, *21*, 8832–8839.
10 H. Shigemitsu, I. Hamachi, *Chem. Asian J.* **2015**, *10*, 2026–2038.
11 M. Rad-Malekshahi, L. Lempsink, M. Amidi, W. E. Hennink, E. Mastrobattista, *Bioconjugate Chem.* **2016**, *27*, 3−18.
12 J. A. A. W. Elemans, S. Lei, S. De Feyter, *Angew. Chem. Int. Ed.* **2009**, *48*, 7298–7332.
13 D. Bonifazi, S. Mohnani, A. Llanes-Pallas, *Chem. Eur. J.* **2009**, *15*, 7004–7025.
14 K. S. Mali, N. Pearce, S. De Feyter, N. R. Champness, *Chem. Soc. Rev.* **2017**, *46*, 2520–2542.
15 R. Matmour, I. De Cat, S. J. George, W. Adriaens, P. Leclère, P. H. H. Bomans, N. A. J. M. Sommerdijk, J. C. Gielen, P. C. M. Christianen, J. T. Heldens, J. C. M. van Hest, D. W. P. M. Löwik, S. De Feyter, E. W. Meijer. A. P. H. J. Schenning, *J. Am. Chem. Soc.* **2008**, *130*, 14576–14583.
16 N. Kalashnyk, J. T. Nielsen, E. H. Nielsen, T. Skrydstrup, D. E. Otzen, E. Lægsgaard, C. Wang, F. Besenbacher, N. C. Nielsen, T. R. Linderoth, *ACS Nano* **2012**, *6*, 6882−6889.
17 S. A. Claridge, J. C. Thomas, M. A. Silverman, J. J. Schwartz, Y. Yang, C. Wang, P. S. Weiss, *J. Am. Chem. Soc.* **2013**, *135*, 18528−18535.
18 X. Mao, Y. Guo, Y. Luo, L. Niu, L. Liu, X. Ma, H. Wang, Y. Yang, G. Wei, C. Wang, *J. Am. Chem. Soc.* **2013**, *135*, 2181−2187.
19 Y. Yang, C. Wang, *Philos. Trans. A Math. Phys. Eng. Sci.* **2013**, 371: 20120311.
20 L. Liu, L. Niu, M. Xu, Q. Han, H. Duan, M. Dong, F. Besenbacher, C. Wang, Y. Yang, *ACS Nano* **2014**, *8*, 9503−9510.
21 Y. Yu, Y. Yang, C. Wang, *Chin. J. Chem.* **2015**, *33*, 24–34.
22 F. Qu, L. Yu, H. Xie, Y. Zheng, J. Xu, Y. Zou, Y. Yang, C. Wang, *J. Phys. Chem. C* **2017**, *121*, 10364−10369.
23 J. L. Zhang, J. Q. Zhong, J. D. Lin, W. P. Hu, K. Wu, G. Q. Xu, A. T. S. Wee, W. Chen, *Chem. Soc. Rev.* **2015**, *44*, 2998–3022.
24 D. Frath, S. Yokoyama, T. Hirose, K. Matsuda, *J. Photochem. Photobiol. C* **2017**, *34*, 29−40.
25 R. Arai, S. Uemura, M. Irie, K. Matsuda, *J. Am. Chem. Soc.* **2008**, *130*, 9371–9379.
26 T. Sakano, Y. Imaizumi, T. Hirose, K. Matsuda, *Chem. Lett.* **2013**, *42,* 1537–1539.
27 S. Yokoyama, T. Hirose, K. Matsuda, *Chem. Commun.* **2014**, *50* 5964–5966.
28 N. Maeda, T. Hirose, S. Yokoyama, K. Matsuda, *J. Phys. Chem. C* **2016**, *120*, 9317–9325.
29 S. Yokoyama, T. Hirose, K. Matsuda, *Langmuir* **2015**, *31*, 6404–6414.
30 N. Katsonis, T. Kudernac, M. Walko, S. J. van der Molen, B. J. van Wees, B. L. Feringa, *Adv. Mater.* **2006**, *18*, 1397–1400.
31 Arramel, T. C. Pijper, T. Kudernac, N. Katsonis, M. van der Maas, B. L. Feringa, B. J. van Wees, *Nanoscale* **2013**, *5*, 9277–9282.
32 M. J. Comstock, N. Levy, A. Kirakosian, J. Cho, F. Lauterwasser, J. H. Harvey, D. A. Strubbe, J. M. J. Fréchet, D. Trauner, S. G. Louie, M. F. Crommie, *Phys. Rev. Lett.* **2007**, *99*, 038301.
33 I. V. Pechenezhskiy, J. Cho, G. D. Nguyen, L. Berbil-Bautista, B. L. Giles, D. A. Poulsen, J. M. J. Fréchet, M. F. Crommie, *J. Phys. Chem. C* **2012**, *116*, 1052–1055.
34 H. Böckmann, S. Liu, J. Mielke, S. Gawinkowski, J. Waluk, L. Grill, M. Wolf, T. Kumagai, *Nano Lett.* **2016**, *16*, 1034–1041.
35 K. Okuyama, R. Somashekar, K. Noguchi, S. Ichimura, *Biopolymers* **2001**, *59*, 310–319.
36 O. A. Gus'kova, P. G. Khalatur, P. Bäuerle, A. R. Khokhlov, *Chem. Phys. Lett.* **2008**, *461*, 64–70.
37 K. Uchida, M. Irie, *Chem. Lett.* **1995**, *24*, 969–970.
38 N. Nishitani, T. Hirose, K. Matsuda, *Chem. Asian J.* **2015**, *10*, 1926–1931.
39 D. Frath, T. Sakano, Y. Imaizumi, S. Yokoyama, T. Hirose, K. Matsuda, *Chem. Eur. J.* **2015**, *21*, 11350–11358.
40 S. Yokoyama, T. Hirose, K. Matsuda, *Chem. Eur. J.* **2015**, *21*, 13569–13576.
41 N. Nishitani, T. Hirose, K. Matsuda, *Langmuir* **2017**, *33*, 9151–9159.
42 N. Maeda, T. Hirose, K. Matsuda, *Angew. Chem. Int. Ed.* **2017**, *56*, 2371–2375.
43 N. Nishitani, T. Hirose, K. Matsuda, *Chem. Lett.* **2019**, *48*, 253–256.



 